Prospecting for rare earth element (hyper)accumulators in the Paris Herbarium using X-ray fluorescence spectroscopy reveals new distributional and taxon discoveries

Léo Goudard, Damien Blaudez, Catherine Sirguey, Imam Purwadi, Vanessa Invernon, Germinal Rouhan, Antony van der Ent

Prospecting for rare earth element (hyper)accumulators in the Paris Herbarium using X-ray fluorescence spectroscopy reveals new distributional and taxon discoveries

Léo Goudard[1], Damien Blaudez[2], Catherine Sirguey[1], Imam Purwadi[3], Vanessa Invernon[4], Germinal Rouhan[4], Antony van der Ent[1,5*]

[1]Université de Lorraine, INRAE, LSE, F-54000, Nancy, France; [2]Université de Lorraine, CNRS, LIEC, F-54000, Nancy, France; [3]Centre for Mined Land Rehabilitation, Sustainable Minerals Institute, The University of Queensland, Brisbane, Australia; [4]Institut de Systématique, Evolution, Biodiversité (ISYEB), Muséum national d'Histoire naturelle, CNRS, Sorbonne Université, École Pratique des Hautes Études, Université des Antilles, Paris, France; [5]Laboratory of Genetics, Wageningen University and Research, The Netherlands.

**For correspondence: antony.vanderent@wur.nl*

ABSTRACT

Context Rare earth elements (REEs) are increasingly crucial for modern technologies. Plants could be used as a biogeochemical pathfinder and a tool to extract REEs from deposits. However, a paucity of information on suitable plants for these tasks exists.

Methods We aimed to discover new REE (hyper)accumulating plant species by performing an X-ray fluorescence (XRF) survey at the Herbarium of the Muséum national d'Histoire naturelle (MNHN, Paris, France). We selected specific families based on the likelihood of containing REE-hyperaccumulating species, based on known taxa that accumulate REEs. A total of 4425 specimens, taken in the two main evolutionary lineages of extant vascular plants, were analysed, of which the two fern families Blechnaceae (*n* 561) and Gleicheniaceae (*n* 1310), and the two flowering plants Phytolaccaceae (n 1137) and Juglandaceae (*n* 1417).

Key results Yttrium (Y) was used as a proxy for REEs for methodological reasons, and a total of 268 specimens belonging to the genera *Blechnopsis* (*n* 149), *Dicranopteris* (*n* 75), *Gleichenella* (*n* 32), *Phytolacca* (*n* 6), *Carya* (*n* 4), *Juglans* (*n* 1), and *Sticherus* (*n* 1) were identified with Y concentrations ranging from the limit of detection (LOD) >49 µg g^{-1} up to 1424 µg g^{-1}. Subsequently, analysis of fragments of selected specimens by inductively coupled plasma atomic emission spectroscopy (ICP-AES) revealed that this translated to up to 6423 µg total REEs g^{-1} in *Dicranopteris linearis* and up to 4278 µg total REEs g^{-1} in *Blechnopsis orientalis* which are among the highest values ever recorded for REE hyperaccumulation in plants. It also proved the validity of Y as an indicator for REEs in XRF analysis of herbarium specimens. The presence of manganese (Mn) and zinc (Zn) was also studied with the XRF in the selected specimens. Mn was detected in 1440 specimens ranging from the detection limit at 116 µg g^{-1} up to 3807 µg g^{-1} whilst Zn was detected in 345 specimens ranging from the detection limit 77 µg g^{-1} up to 938 µg g^{-1}.

Conclusions & Implications This study led to the discovery of REE accumulation in a range of plant species, substantially higher concentrations in species known to be REE hyperaccumulators, and records of REE hyperaccumulators outside of the well-studied populations in China.

Keywords: *hyperaccumulators; phylogenetic diversity; XRF technology.*

INTRODUCTION

Global herbarium collections are among the most important sources of information for acquiring ionomic, taxonomic, genetic, and biogeographic data in the plant kingdom (Greve et al., 2016; Souza and Hawkins, 2017; Heberling et al., 2019; van der Ent et al., 2019 a). The term "ionome" refers to the entirety of elements found in plants, including metallic, metalloid, and non-metallic elements (Lahner et al., 2003). The terms "metallome" or "elementome" specifically refer to the total composition of metallic or non-metallic elements in a plant (Edwards et al., 2014; Peñuelas et al., 2019). To characterize the complete ionome or metallome of an herbarium plant, a non-destructive analytical method is necessary to preserve the integrity of the specimens. Portable X-ray fluorescence (XRF) spectroscopy fulfills this requirement by emitting high-energy X-rays onto a localized area of the plant (van der Ent et al., 2019 b). The elements in the radiation zone are excited and in return emit characteristic fluorescent X-rays. Our research builds upon previous studies that utilized portable XRF to obtain elemental data from herbarium specimens (van der Ent et al., 2019 b; Do et al., 2020; Gei et al., 2020). In our case, the main elements of interest in herbarium plants are the rare earth elements (REEs). Their presence is detected using the yttrium (Y) as a proxy for REEs. The choice of Y as a proxy is due to the fact that the most abundant REEs in plants (lanthanum (La) and neodymium (Nd)) emit relatively weak L-lines that are indistinguishable from the K-lines produced by transition elements titanium (Ti) to manganese (Mn). Furthermore, the energy generated by the X-ray source (with an Ag-anode) optimally excites the Y Kα-line, producing no interference and allowing very sensitive detection (van der Ent et al., 2023). This approach has been employed in a recent study conducted on Queensland herbarium specimens, revealing anomalously high Y concentrations (>1000 µg g^{-1}) in the genus *Helicia* (Proteaceae) (Purwadi et al., 2023).

Rare earth elements (REEs) are a group of seventeen chemical elements: fifteen lanthanides (atomic numbers (Z) from 57 to 71) plus yttrium (Z = 39) and scandium (Z = 21). They have similar physical and chemical properties and are typically found in the same minerals. REEs can be divided into two subgroups based on their atomic mass and effective radius: La, Ce, Pr, Nd, Pm, Sm, and Eu are classified as light REEs (LREEs), whereas Gd, Tb, Dy, Ho, Er, Tm, Yb, Lu, Sc and Y are classified as heavy REEs (HREEs). REEs are characterized by their low concentration in pure ore deposits and their great importance for modern industry, particularly in energy,

telecommunications, electric motors, permanent magnets, and lasers (Balaram, 2019). The increasing demand for these metals raises concerns about their environmental and social impact (Rim, 2016). Studies on REE hyperaccumulating plants are still limited, but it has been shown that they may be used to recover these metals from REE mine tailings and REE geochemical anomalous soils (van der Ent et al., 2021).

Hyperaccumulating plants are able to accumulate metallic elements at extremely high concentrations in their leaves (Reeves et al., 1999). Hyperaccumulation is a rare phenomenon that occurs in about 0.2% of total angiosperms (Reeves et al., 2018). Currently, about 700 hyperaccumulators of various metals have been catalogued in the world. Of these, only 21 (hyper)accumulate REEs (Liu et al., 2021a; van der Ent et al., 2021). Several studies have observed correlations between the uptake of REEs and that of macro-micro-elements (Fe, Mg, Ca, Mn, Al, Zn) by plants. One hypothesis explaining this phenomenon would be the existence of common pathways for the accumulation of REEs and several essential elements (Grosjean et al., 2020; Liu et al., 2021 a; van der Ent et al., 2023). The threshold concentration for REE hyperaccumulation is not yet unambiguously defined, but ranges from 100 to 1000 µg g^{-1} (van der Ent et al., 2021). The fern *D. linearis* (Gleicheniaceae) has been found in China to accumulate La, Ce, Pr, and Nd at 7000 µg g^{-1} in total of dry matter (Shan et al., 2003). In China, the fern species *Blechnopsis orientalis* (as *Blechnum orientale;* Blechnaceae) and *Grypothrix simplex* (as *Pronephrium simplex*; Thelypteridaceae) are known to respectively accumulate 1047 µg g^{-1} REEs and 3000 µg g^{-1} REEs in their leaves respectively (Lai et al., 2006; Liu et al., 2021 a; Wang et al., 2023). In the USA, trees of the genus *Carya* (Juglandaceae), with the species *C. tomentosa* and *C. glabra*, have also shown a remarkable ability to accumulate REEs, with total REEs concentrations of 1350 µg g^{-1} for the former and 2300 µg g^{-1} for the latter (Robinson et al., 1958; Thomas, 1975). More recently, the herbaceous plant *Phytolacca americana* (Phytolaccaceae), growing naturally near an REE mine in China, had a total leaf concentration of 1040 µg REEs g^{-1} (Yuan et al., 2018).

The objective of this study was to increase the inventory of plant species hyperaccumulating REEs, by identifying new species containing abnormally high concentrations of REEs in their leaves. The portable XRF instrument also allows for obtaining the concentrations of other elements in the measured specimens. Therefore, a secondary objective of this study was to investigate a potential correlation between the foliar accumulation of REEs and foliar accumulation of Mn and Zn. To

attain this aim, handheld XRF scanning was performed at the Herbarium of Muséum national d'Histoire naturelle (MNHN, Paris, France).

MATERIALS AND METHODS

Selection of herbarium specimens for the XRF scanning

In order to carry out this study, it was necessary to make a preliminary selection based on specimens from the Herbarium of the Muséum national d'Histoire naturelle (MNHN, Paris, France). This herbarium holds the world's largest collection of plants, with over 8 million specimens from all five continents (Le Bras et al., 2017). A selection at the family level represented too many specimens to scan, so it was decided to limit the selection to the genus level. In the end, 12 genera representing the two main evolutionary lineages of extant vascular plants (the ferns *Blechnopsis*, *Dicranopteris Gleichenella* and *Sticherus*; the angiosperms *Annamocarya*, *Carya*, *Engelhardtia*, *Juglans*, *Phytolacca*, *Platycarya*, *Pterocarya*, and *Rhoiptelea*), belonging to four plant families (Blechnaceae and Gleicheniaceae for the ferns, Juglandaceae and Phytolaccaceae in angiosperms) were selected on the basis of knowledge, for a total of 4425 specimens analysed during this study. Each specimen is identified with a unique and non-equivocal sample number (PXXXXXXXX), ensuring its traceability and the repeatability of analyses performed at the MNHN.

Handheld XRF calibration and data processing

A Thermo Fisher Scientific Niton^{TM} XL3t 950 GOLDD+ portable XRF instrument was used in 'Soils Mode' coupled with the 'Main filter' at 50 kV aiming to excite K-shell of first row transition metals. The elements targeted in the specimens analysed by XRF were Y, which served as a tracer for the presence of REEs, as well as Mn and Zn. Each specimen was placed on two pure (99.995%) 2 mm thick plates of titanium and molybdenum and measured for 30 s. This setting was used to absorb X-rays transmitted through the specimen and to ensure a uniform background. Each specimen was measured once only at leaf lamina. This procedure produces errors of less than 4% compared to the mean concentration of the whole leaf for the first-row transition metals (Purwadi et al., 2022). The obtained spectra were processed in GeoPIXE 7.5, a software package based on Dynamic Analysis that has been developed for synchrotron-based XRF and nuclear microprobe

techniques (Ryan, 2000; Ryan et al., 2005). The instrument was calibrated in a previous study (Purwadi et al., 2022) to obtain relevant instrumental parameters (filter material and thickness, source composition, detector dimensions, *etc*.) required by GeoPIXE. The Dynamic Analysis method is a Fundamental Parameter approach that solves complex physics equations (Sherman, 1955) by iteratively fitting linear and non-linear models to decompose the full XRF spectrum to a single spectrum of each element within the sample that contributes to the full XRF spectrum (Ryan, 2000; Ryan et al., 2005, 2015). The LODs for these elements, determined by GeoPIXE analysis of sample spectra, ranged from 49 µg g^{-1} to 73 µg g^{-1} for Y, 115 µg g^{-1} to 165 µg g^{-1} for Mn, and 77 µg g^{-1} to 113 µg g^{-1} for Zn. For all three elements, concentrations >LOD were observed in each family. Taking the prevailing Y concentrations in *D. linearis* (Wei et al., 2005; Liu et al., 2020; van der Ent et al., 2023), *Helicia* species (herbarium specimens) (van der Ent et al., 2023) and *Carya* species (Wood et al., 2011) compared to tREEs yields a range of 1.3–20.2% of the total of tREEs, taking the mean Y (9.9%) and established tREE hyperaccumulation threshold (1000 µg g^{-1}) this translates to a Y hyperaccumulation threshold of 99 µg g^{-1}. Given the uncertainty about the REE hyperaccumulation phenomenon, considering normal background concentrations of <5 µg g^{-1} Y and to avoid missing potential REE hyperaccumulators with a low Y to REE ratio, we take half this value and refer to plants as Y hyperaccumulators if exceeding 50 µg g^{-1} Y.

Destructive sample analysis with ICP-AES

Analyses were performed on 10 specimens identified with high foliar concentrations of Y based on XRF analysis (*Blechnopsis orientalis* n = 4; *Dicranopteris linearis n* = 3; *Dicranopteris flexuosa* n = 2; *Gleichenella pectinata n* = 1). The measured samples represent a leaf section of approximately 2 cm^2 from the identified specimens. They were finely ground (<250 µm) and weighed at 0.05 g (± 0.005 g), except for samples P01315862, P01571495, P01315958, and P01474002 where the plant material was insufficient. The dried plant material was digested in an HNO_3 + H_2O_2 mixture (1:3, v:v) for 16 hours at room temperature before heating at 95°C for 2 hours in a graphite heating block (DigiPREP® system, SCP Science, Baie-d'Urfé, QC, Canada). After filtration at 0.45 µm, the plant samples were analysed using induced coupled plasma atomic emission spectrometry (ICP-AES, iCAP 6000 series, Thermo Scientific, Cambridge, UK) to measure the concentrations of REEs and other elements as Mn and Zn. For quality control, a

certified reference sample (BCR-670, *Lemna minor*) and an internal control sample (LSE-EchCont-20, *Noccaea caerulescens*) with known values were used.

Synchrotron µXRF experiments

The X-ray fluorescence microscopy experiments were undertaken at PETRA III (Deutsches Elektronen-Synchrotron DESY), a 6 GeV synchrotron radiation source, specifically at the hard X-ray microprobe undulator beamline P06 (Boesenberg et al., 2016). P06 is equipped with a cryogenically cooled double-crystal monochromator with Si(111) crystals. Using different focusing optics, the X-ray beam can be focused down to sub-micron level. An ion chamber upstream of the sample is used to monitor the incoming flux, while a 500 µm thick Si PIPS diode with a 19 mm diameter active area (PD300-500CB, Mirion Technologies (Canberra) GmbH, Germany) located downstream of the sample can be used to record the transmitted X-ray intensity in order to extract absorption data. Multiple XRF detectors allow for the measurement of X-ray fluorescence data. The incident X-ray energy was 18 keV for the whole experiment and focussed with K-B mirrors to 3.57 × 0. 92 µm (h × v), resulting in a flux of about 1.25^{11} ph/s in the focus. For XRF detection, both a Vortex ME4 in ~45° geometry with detector-sample distance ~5.5 cm and a prototype 16-element SDD Ardesia detector (800 µm thick chip with about 324 mm^2 combined active area for all 16 elements, Politecnico Milano, Italy (Utica et al., 2021) in 315° geometry with detector-sample distance ~6.0 cm with Xspress 3 pulse processors were used.

Data presentation and analysis

The elemental concentrations reported by GeoPIXE were processed further in R v4.1.1 and RStudio v1.4.1106. Dunn's Kruskal-Wallis post-hoc test was performed to check the similarity in elemental distribution across the family by using 'FSA' package ($P \leq 0.05$). For data analysis, all graphs in this study were created using RStudio V4.0.2 and the "ggplot2" package. The violins charts were generated using analytical data that included only specimens with detection values for the elements of interest (Y, Mn, Zn) above the limits of detection (>LOD). The same data was also used to create vertical and horizontal bar plots. The x-axis scale of the vertical bar plots was transformed into log10. The skewness of the distributions was assessed using the skewness test from the 'PerformanceAnalytics' package on Rstudio. Hartigan's dip test was performed for each vertical bar plot, except for Y with the Juglandaceae (n = 5) and Phytolaccaceae (n = 6) families

due to the insufficient number of values. This test was used to assay the unimodality in the frequency distributions with the "dip test" package in RStudio. The horizontal bar plots show the number of analysed specimens belonging to different accumulation levels (normal, accumulator and non-accumulator) for Y, Mn, and Zn defined from the literature (Table 1). The heatmap was generated based only on species with at least one specimen with a Y-value >LOD. The percentages shown indicate the proportion of specimens with detection values >LOD compared to the total number of specimens analysed in this study for a given species and a given element of interest (Y, Mn, Zn). In order to validate the method used in this study, a linear regression was applied to compare the Y concentrations obtained by ICP-AES with those obtained by the handheld XRF. To this end, 10 samples that handheld XRF measured with low, medium, and high Y concentrations were selected and destructively sampled (Suppl Fig 1). Each specific sample was first measured twice with handheld XRF, and acid digested and analysed by ICP-AES. A Pearson test was carried out confirming a positive correlation between these two modes of measurement (Pearson correlation 0.84, *P* 0.0022). The synchrotron µXRF event stream was processed using non-linear least-squares fitting as implemented in PyMCA (Solé et al., 2007). The figures were prepared in ImageJ (Schneider et al., 2012) by changing the LUT to 'Fire' and adjusting of the maximum values and adding length scales.

RESULTS

Overall observations on the handheld XRF dataset

This study analysed 142 species (Suppl Table 1) from 12 genera, belonging to four plant families, for a total of 4425 scanned specimens. It should be noted that this study did not examine the entire genera of each family mentioned above, but only the 12 genera mentioned. Hence, the results presented at the family level were not exhaustive for these families but referred only to specimens belonging to the specific genera. However, all specimens belonging to these genera and present at the MNHN in Paris were analysed using handheld XRF, except for the genus *Blechnopsis*, for which only one species, *B. orientalis*, was analysed. The elements of interest in this study were Y, Mn, and Zn. Y was detected in a total of 268 specimens (6.1% of total specimens scanned) belonging to 16 species and 7 genera (Table 2). Mn concentrations >LOD was found in 1440

specimens (32.5%) belonging to 97 species and 12 genera, and 345 specimens (7.8%), belonging to 64 species and 9 genera presented Zn concentrations >LOD.

General description of the distribution of Y, Mn, and Zn concentrations among families

Violin charts show the distribution of specimens according to their concentrations of elements of interest (Y, Mn, Zn) based on the family to which they belong (Fig 1). Among the four families studied, the Blechnaceae family represented 56% (*n* 149) of the total number of specimens with leaf Y concentrations >LOD. The foliar Y concentrations measured in this family were the most dispersed with values ranging from 49 μg g^{-1} to 1424 μg g^{-1}. A lower dispersion was found in the Gleicheniaceae, for which 108 specimens (40%) were found with foliar Y concentrations ranging from 49 μg g^{-1} to 697 μg g^{-1}. In the other two families, only five specimens (2%) from the Juglandaceae had foliar Y concentrations ranging from 56 μg g^{-1} to 205 μg g^{-1}, and six specimens (2%) from the Phytolaccaceae had foliar Y concentrations ranging from 59 μg g^{-1} to 94 μg g^{-1}. The distribution of Y concentrations observed among families is related to the relatively high LOD value of Y with the XRF instrument (49 μg g^{-1}) and only specimens with exceptional Y concentrations could be identified here.

For Mn and Zn, the four families also showed different dispersion profiles, but with an opposite pattern. Thus, the Phytolaccaceae showed the greatest variability for both elements. For Mn, concentrations ranged from 116 μg g^{-1} to 3807 μg g^{-1} for a total of 354 specimens (25%), and for Zn concentrations ranged from 78 μg g^{-1} to 938 μg g^{-1} for a total of 148 specimens (43%). The dispersion was slightly lower in the Juglandaceae. Of a total of 582 specimens (40%), Mn concentrations ranged from 116 μg g^{-1} to 3265 μg g^{-1}. For Zn, 125 specimens (36%) were measured with foliar concentrations ranging from 77 μg g^{-1} to 691 μg g^{-1}. With a similar shape, the Gleicheniaceae had a lower variability. Of a total of 477 specimens (33%), Mn concentrations ranged from 116 μg g^{-1} to 2644 μg g^{-1}. For Zn, concentrations ranged from 77 μg g^{-1} to 567 μg g^{-1} for a total of 52 specimens (15%). Finally, the Blechnaceae had the lowest variability with 27 specimens (2%) with Mn concentrations ranging from 121 μg g^{-1} to 522 μg g^{-1} and 20 specimens (6%) with Zn concentrations ranging from 84 μg g^{-1} to 402 μg g^{-1}.

(Hyper)accumulation potential of Y, Mn, and Zn at the family level

The frequency distribution and the density curve for Y concentrations in the herbarium specimens (Fig 2.A) were positively skewed for the Blechnaceae and the Gleicheniaceae families with a tail spreading to the right. For both families, the majority of specimens with Y values >LOD (69% and 66%, respectively) had concentrations below their mean concentrations (179 µg g^{-1} and 141 µg g^{-1}, respectively). Skewness tests confirmed the positive skewness of both distributions (2.16 and 3.61) with however, an unimodality of both datasets confirmed by Hartigans' dip tests (p = 0.75 and p = 0.95). In total, 147 plant specimens from the Blechnaceae and 107 plant specimens from the Gleicheniaceae had Y foliar concentrations > 50 µg g^{-1}, making them Y hyperaccumulators (Fig 2.B). The numbers of specimens from the Juglandaceae and Phytolaccaceae with Y values above LOD were too low to identify a trend in the frequency distribution of Y concentrations. However, all of these specimens, respectively 5 and 6 may be considered as hyperaccumulators.

The frequency distribution of Mn and Zn concentrations in the herbarium specimens were positively skewed with a tail spreading to the right for the four families studied (Fig 3.A). This was confirmed by skewness tests which were all significantly greater than 1 for both Mn and Zn and the four families. These distributions were also unimodal distributions, which were confirmed by Hartigans' dip tests whose p-values were much above 0.05 for each distribution. Of the 1440 specimens with Mn values >LOD, 322 were between 500 µg g^{-1} and 3000 µg g^{-1} and considered as Mn accumulators. This included two specimens from the Blechnaceae, 64 from the Gleicheniaceae, 164 from the Juglandaceae, and 92 from the Phytolaccaceae (Fig 3.B). None of the scanned specimens were above the hyperaccumulation threshold for Mn (3000 µg g^{-1}). Finally, of the 345 specimens with Zn values >LOD, 72 were between 200 µg g^{-1} and 3000 µg g^{-1} and considered as Zn accumulators. This included 4 specimens from the Blechnaceae, 14 from the Gleicheniaceae, 16 from the Juglandaceae, and 42 from the Phytolaccaceae (Fig 3.B).

(Hyper)accumulation potential of Y, Mn, and Zn at the species level

Among the 12 plant genera analysed in this study, seven contained a total of 268 specimens with Y concentrations >LOD in their leaves: *Blechnopsis* (n = 149), *Dicranopteris* (n = 75), *Gleichenella* (n = 32), *Phytolacca* (n = 6), *Carya* (n = 4), *Juglans* (n = 1), and *Sticherus* (n = 1) (Fig 4). Of these specimens, 265 were hyperaccumulators of Y and were distributed among 16

species as shown in Figure 4. In the 'hyperaccumulator' category, the species *B. orientalis* contained 147 specimens (26% of the specimens scanned for this species) of the *Blechnopsis* genus knowing that *B. orientalis* is the only species (out of two recognized) scanned for this genus. For *Dicranopteris*, 57 specimens (7%) belonged to *D. linearis* and 13 (10%) to *D. flexuosa* and for *Gleichenella* 32 (13%) to *G. pectinate*. The remaining specimens (*n* 7) are distributed among the following species: *S. bifidus*, *D. cadetii*, *D. nervosa*, and *D. splendida*. For *Phytolacca*, the 6 specimens hyperaccumulating Y were distributed among the four species *P. decandra*, *P. dioica*, *P. octandra*, and *P. rivinoides*. For *Carya*, the four specimens were distributed among *C. minima*, *C. pallida*, and *C. porcina*. Finally, one specimen of *Juglans nigra* was identified as an Y hyperaccumulator. Among the 16 species with foliar Y concentrations >LOD, 556 and 108 specimens were found respectively as normal and accumulator plants regarding their foliar Mn concentrations. These latter were distributed in four genera: *Dicranopteris* (*n* = 61), *Phytolacca* (*n* = 27), *Carya* (*n* = 16), *Gleichenella* (*n* = 2), and *Blechnopsis* (n = 2). Finally, for Zn and still on the basis of the 16 species mentioned above, 116 plant specimens had 'normal' foliar Zn concentrations, and 37 were identified as Zn accumulators. These 37 specimens were distributed in three genera: *Phytolacca* (*n* = 23), *Dicranopteris* (*n* = 7), *Blechnopsis* (*n* = 4), *Gleichenella* (*n* = 3).

Focus on high range Y species (B. orientalis, D. linearis, D. flexuosa and G. pectinata)

The concentrations of REEs and other elements obtained by ICP-AES for *B. orientalis* (n = 4), *D. linearis* (*n* = 3), *D. flexuosa* (*n* = 2), and *G. pectinata* (*n* = 1) are shown in Table 3 and Table 4. The highest concentration of REEs was found in *D. linearis*, with a total of 6423 µg g^{-1}. In *B. orientalis*, all four samples had REEs concentrations above 2000 µg g^{-1}, with a maximum of 4278 µg g^{-1}. Finally, 2780 µg g^{-1} and 1447 µg g^{-1} of REEs were found in *D. flexuosa* and *G. pectinata*, respectively. Yttrium was the most accumulated REE in these 10 plant samples (24%), and light REEs (LREEs) were present in much higher concentrations than heavy REEs (HREEs).

Synchrotron µXRF analysis

Synchrotron µXRF was used to investigate whether there was any surgical contamination on the specimens that could have influenced the results of the handheld XRF scanning, and to provide information about the distributed of the REEs in the tissues. For this purpose, a specimen

(P01523962) with high Y (1032 µg g^{-1} by handheld XRF) was selected and a 10 cm frond fragment extracted. An overview scan (Fig 5) reveals that Ce in concentration in the vascular bundles of the pinnules, and the distributions of La and Nd are similar, whilst Y is also enriched in the areas surrounding the veins. There is notable enrichment in the margins of the pines, but this likely results from the curling of the pinnules edges. A high-resolution scan of the single pinnule (Fig 6) provides further detail on these distributions and shows that the REEs (Ce, La, N, Pr) have similar distributions with localisation in the secondary vascular bundles and some minor (necrotic) hotspots. The disputations of light (K, Ca) and transition elements (Fe, Mn, Zn) as well of that of Br and Rb are also provided (Fig 6, Suppl Fig 2, Suppl Fig 3). Very low Fe concentrations and absence of hotspot specks (*e.g.,* soil particles) strongly suggest that surgical contamination is negligible. The distribution of Br highlights the sporangia in the pinnule smartens.

DISCUSSION

The herbarium XRF scanning is an effective method that can be used to discover new metal/metalloid (hyper)accumulator plant species in herbaria (Nkrumah et al., 2018; van der Ent et al., 2019 a; Gei et al., 2020). This approach enabled to measure 4425 specimens held in the MNHN in Paris in search of novel REE (hyper)accumulators led to amongst the highest values for REE hyperaccumulation in plants: *D. linearis* is 6423 µg g^{-1}. In this study, for methodological reasons, Y was used as a proxy for REEs. For example, Y represents 6% of the total REEs accumulated by *D. linearis* growing on ion adsorption REE mine tailings in China (Liu et al., 2020) and 24% of the total REEs present in the 10 plant samples analysed by ICP-AES in this study.

The XRF scanning results show that 147 specimens of *B. orientalis* and 56 specimens of *D. linearis* accumulate Y in their leaves up to concentrations of 1424 µg g^{-1} and 697 µg g^{-1}, respectively. *Dicranopteris linearis* is a fern already widely documented for its REE (hyper)accumulation capabilities in the locations in China, but is in fact, polyphyletic, representing a species complex of cryptic species (Wei et al., 2022; Vieira Lima et al., 2023). This study reveals some specimens of *D. linearis* accumulating more than 1000 µg g^{-1} of REEs in their fronds are from Indonesia and the Philippines, but these populations may well represent distinct species within the *D. linearis* complex. Although much less studied than *D. linearis,* another fern from a different family

(Blechnaceae), *B. orientalis* has been shown by Zhang et al. (2004) and Wang et al. (2023) to be capable of accumulating up to 865–1047 µg g^{-1} total REE elements. This study shows that a significant portion of the analysed *B. orientalis* specimens accumulates high concentrations of Y, which is confirmed by the ICP-AES analyses with a concentration of total REEs reaching 4278 µg g^{-1} in a specimen. Therefore, further studies on the potential of *B. orientalis* as a REE hyperaccumulator should be conducted to confirm its REE accumulation capabilities and determine its bioconcentration factor. Furthermore, this study shows that *B. orientalis* and *D. linearis* have accumulated high concentrations of REEs outside of the known REE ion exchange deposits in China. This is relevant because REE hyperaccumulation has previously mainly been identified in these REE-enriched areas. Discovery of REE hyperaccumulators in Indonesia and the Philippines may lead to the discovery of new deposits present in these countries, by using them as a pathfinder for REE deposits.

Previous research has identified correlations between the uptake of REEs by plants and that of certain micronutrients. For instance, Wood and Grauke (2011) reported a positive relationship between the accumulation of Mg, Ca, Mn, and Fe and the foliar concentrations of REEs in *Carya*. Similarly, Liu et al. (2021 b) found a positive association between the accumulation of REEs and the foliar concentrations of Al, Fe, and Zn in *Phytolacca americana*. In several fern genera, such as those examined by Grosjean et al. (2020), foliar REE concentrations were also positively correlated with the uptake of multiple microelements. In our study, however, we did not observe any correlation between Y and Mn or Zn, only 18 specimens accumulated Y and Mn and six accumulated Y and Zn which may be due to differences in the leaf distribution of these elements as well as to the high LODs values of our instrument.

Furthermore, this study led to the discovery of 15 additional plant species that are potential REE hyperaccumulators, these are the trees *Carya minima*; *C. pallida*, *C. porcina* and *Juglans nigra*, the ferns *Gleichenella pectinata*; D*icranopteris cadetti*; D. *flexuosa*; *D. nervosa*; *D. splendida*, *Sticherus bifudus* and the Dicot herbs *Phytolacca decandra*, *P. dioica*, *P. octandra* and *P. rivinoides*. Surprisingly, no specimens of *Carya tomentosa* and *Phytolacca americana* were identified with foliar Y concentrations >LOD, even though these species are known to accumulate more than 1000 µg g^{-1} of REEs in their leaves (Thomas, 1975; Liu et al., 2020). However, the minimum concentrations obtained in this study are limited by the LOD value of Y (47 µg g^{-1}). This

value is much higher than the concentrations normally present in plants, which results in exceptional specimens being highlighted at the expense of normal and abnormal specimens.

CONCLUSIONS

Rare earth element hyperaccumulation is a prevalent phenomenon in spore-bearing vascular plants ('Pteridophytes') species. To date, no genus has been evidenced in the lycophytes, and 17 genera identified with species that can accumulate REEs in their leaves are ferns: *Adiantum*, *Alsophila*, *Asplenium*, *Athyrium*, *Austroblechnum* and *Blechnopsis* (analysed as *Blechnum* spp. s.l. in former studies), *Cystopteris*, *Christella* (as *Cyclosorus*), *Dicranopteris*, *Diplazium*, *Dryopteris*, *Gleichenella*, *Gleichenia*, *Grypothrix* (as *Pronephrium*), *Odontosoria* (as *Stenoloma*), *Onoclea*, *Polystichum*, *Pteridium*, *Sticherus*, and *Woodwardia* (Ichihashi et al., 1992; Ozaki et al., 2000; Zhang et al., 2004; Lai et al., 2005; Grosjean et al., 2020; Chen et al., 2022). Therefore, it appears that ferns possess a trait that allows them to accumulate high concentrations of REEs. The reasons for this phenomenon are not yet known, but one possibility is that it allows ferns to have greater resilience in their environment (Grosjean et al., 2020) even if many other ferns are considered as bioindicators in being susceptible to environmental changes (Silva et al., 2018). Moreover, among the 22 *Dicranopteris* species analysed in the present study, seven in addition to *D. linearis* could be potential REEs accumulators. Wood and Grauke (2011) reported the presence of a trait for REEs accumulation in *Carya* species, which all accumulate REEs in their leaves. Grosjean et al. (2020) reported high REEs accumulation in *Athyrium* species, unlike *Polypodium* species, which are lower level accumulators. The conservation of this trait for REE accumulation within 'Pteridophytes' genera could lead to the discovery of numerous additional REE (hyper)accumulating species. The usefulness of Y as an indicator for REEs in XRF analysis of herbarium specimens was proven in this study.

DATA AVAILABILITY STATEMENT

The data that supports this study will be shared upon reasonable request to the corresponding author.

ACKNOWLEDGMENTS

We thank the MNHN for giving us access to the collections in the framework of the RECOLNAT national Research Infrastructure. We thank Lucas Charrois and Romain Goudon (University of Lorraine) for support with the ICP-AES analysis. We acknowledge DESY (Hamburg, Germany), a member of the Helmholtz Association HGF, for the provision of experimental facilities. Parts of this research were carried out at PETRA III and we would like to thank Dennis Bruckner, Gerald Falkenberg and Jan Garrevoet for assistance in using beamline P06. The beamtime was allocated for proposal I-20220755 EC.

FUNDING

This work was supported by the French National Research Agency through the national program "Investissements d'avenir" (ANR-10-LABX-21 - RESSOURCES21).

AUTHOR CONTRIBUTIONS

LG performed the herbarium XRF scanning. IP processed the XRF data. All the authors contributed to the writing of this manuscript.

CONFLICTS OF INTEREST

The authors declare no conflicts of interest relevant to the content of this manuscript.

REFERENCES

Balaram V. 2019. Rare earth elements: A review of applications, occurrence, exploration, analysis, recycling, and environmental impact. Geoscience Frontiers 10:1285–1303. DOI:10.1016/j.gsf.2018.12.005

Boesenberg U, Ryan CG, Kirkham R, et al. 2016. Fast X-ray microfluorescence imaging with submicrometer-resolution integrating a Maia detector at beamline P06 at PETRA III. Journal of Synchrotron Radiation 23:1550–1560. DOI:10.1107/S1600577516015289

Chen H, Chen H, Chen Z. 2022. A review of in situ phytoextraction of rare earth elements from contaminated soils. International Journal of Phytoremediation 24:557–566. DOI:10.1080/15226514.2021.1957770

Do C, Abubakari F, Remigio AC, et al. 2020. A preliminary survey of nickel, manganese and zinc (hyper)accumulation in the flora of Papua New Guinea from herbarium X-ray fluorescence scanning. Chemoecology 30:1–13. DOI:10.1007/s00049-019-00293-1

Edwards NP, Manning PL, Bergmann U, et al. 2014. Leaf metallome preserved over 50 million years. Metallomics 6:774–782. DOI:10.1039/c3mt00242j

Gei V, Isnard S, Erskine PD, et al. 2020. A systematic assessment of the occurrence of trace element hyperaccumulation in the flora of New Caledonia. Botanical Journal of the Linnean Society 194:1–22. DOI:10.1093/botlinnean/boaa029

Greve M, Lykke AM, Fagg CW, et al. 2016. Realising the potential of herbarium records for conservation biology. South African Journal of Botany 105:317–323. DOI:10.1016/j.sajb.2016.03.017

Grosjean N, Blaudez D, Chalot M, Gross EM, Le Jean M. 2020. Identification of new hardy ferns that preferentially accumulate light rare earth elements: a conserved trait within fern

species. Environmental Chemistry 17(2):191–200.
DOI:10.1071/EN19182

Heberling JM, Prather LA, Tonsor SJ. 2019. The Changing Uses of Herbarium Data in an Era of Global Change: An Overview Using Automated Content Analysis. BioScience 69:812–822.
DOI:10.1093/biosci/biz094

Ichihashi H, Morita H, Tatsukawa R. 1992. Rare earth elements (REEs) in naturally grown plants in relation to their variation in soils. Environmental Pollution 76:157–162.
DOI:10.1016/0269-7491(92)90103-H

Lahner B, Gong J, Mahmoudian M, et al. 2003. Genomic scale profiling of nutrient and trace elements in *Arabidopsis thaliana*. Nature Biotechnology 21:1215–1221.
DOI:10.1038/nbt865

Lai Y, Wang Q, Yan W, Yang L, Huang B. 2005. Preliminary study of the enrichment and fractionation of REEs in a newly discovered REE hyperaccumulator *Pronephrium simplex* by SEC-ICP-MS and MALDI-TOF/ESI-MS. Journal of Analytical Atomic Spectrometry 20:751–753.
DOI:10.1039/b501766a

Lai Y, Wang Q, Yang L, Huang B. 2006. Subcellular distribution of rare earth elements and characterization of their binding species in a newly discovered hyperaccumulator *Pronephrium simplex*. Talanta 70:26–31.
DOI:10.1016/j.talanta.2005.12.062

Le Bras G, Pignal M, Jeanson ML, et al. 2017. The French Muséum national d'histoire naturelle vascular plant herbarium collection dataset. Scientific Data 4:170016.
DOI:10.1038/sdata.2017.16

Liu C, Yuan M, Liu W-S, et al. 2021a. Element Case Studies: Rare Earth Elements. In: van der Ent A, Baker AJM, Echevarria G, Morel JL eds. Agromining: Farming for Metals, Mineral Resource Reviews. Springer International Publishing: Cham, 471–483

Liu C, Liu W-S, van der Ent A, et al. 2021b. Simultaneous hyperaccumulation of rare earth elements, manganese and aluminum in *Phytolacca americana* in response to soil properties. Chemosphere 282:131096.
DOI:10.1016/j.chemosphere.2021.131096

Liu W-S, van der Ent A, Erskine PD, et al. 2020. Spatially Resolved Localization of Lanthanum and Cerium in the Rare Earth Element Hyperaccumulator Fern *Dicranopteris linearis* from China. Environ Sci Technol 54:2287–2294.
DOI:10.1021/acs.est.9b05728

Nkrumah PN, Echevarria G, Erskine PD, van der Ent A. 2018. Nickel hyperaccumulation in *Antidesma montis-silam*: from herbarium discovery to collection in the native habitat. Ecological Research 33:675–685.
DOI:10.1007/s11284-017-1542-4

Ozaki T, Enomoto S, Minai Y, Ambe S, Makide Y. 2000. A survey of trace elements in pteridophytes. Biological Trace Element Research 74:259–273.
DOI:10.1385/BTER:74:3:259

Peñuelas J, Fernández-Martínez M, Ciais P, et al. 2019. The bioelements, the elementome, and the biogeochemical niche. Ecology 100:1–15.
DOI:10.1002/ecy.2652

Purwadi I, Casey LW, Ryan CG, Erskine PD, van der Ent A. 2022. X-ray fluorescence Spectroscopy (XRF) for analysis of the Ionome of herbarium specimens. Plant Methods 18:139.
DOI:10.1186/s13007-022-00958-z

Purwadi I, Abubakari F, Brown GK, Erskine PD, van der Ent A. 2023. A systematic assessment of the metallome of selected plant families in the Queensland (Australia) flora by using X-ray fluorescence spectroscopy. Australian Journal of Botany 71(4):199–215.
DOI:10.1071/BT22028

Reeves RD, Baker AJM, Borhidi A, Berazaín R. 1999. Nickel Hyperaccumulation in the Serpentine Flora of Cuba. Annals of Botany 83:29–38.
DOI:10.1006/anbo.1998.0786

Reeves RD, Baker AJM, Jaffré T, Erskine PD, Echevarria G, van der Ent A. 2018. A global database for plants that hyperaccumulate metal and metalloid trace elements. New Phytologist 218:407–411.
DOI:10.1111/nph.14907

Rim K-T. 2016. Effects of rare earth elements on the environment and human health: A literature review. Toxicology and Environmental Health Sciences 8:189–200.
DOI:10.1007/s13530-016-0276-y

Robinson WO, Bastron H, Murata KJ. 1958. Biogeochemistry of the rare-earth elements with particular reference to hickory trees. Geochimica et Cosmochimica Acta 14:55–67.
DOI:10.1016/0016-7037(58)90093-0

Ryan CG. 2000. Quantitative trace element imaging using PIXE and the nuclear microprobe. International Journal of Imaging Systems and Technology 11:219–230.
DOI:10.1002/ima.1007

Ryan CG, Etschmann BE, Vogt S, et al. 2005. Nuclear microprobe - Synchrotron synergy: Towards integrated quantitative real-time elemental imaging using PIXE and SXRF. Nuclear Instruments and Methods in Physics Research Section B: Beam Interactions with Materials and Atoms 231:183–188.
DOI:10.1016/j.nimb.2005.01.054

Ryan CG, Laird JS, Fisher LA, Kirkham R, Moorhead GF. 2015. Improved Dynamic Analysis method for quantitative PIXE and SXRF element imaging of complex materials. Nuclear Instruments and Methods in Physics Research Section B: Beam Interactions with Materials and Atoms 363:42–47.
DOI:10.1016/j.nimb.2015.08.021

Schneider CA, Rasband WS, Eliceiri KW. 2012. NIH Image to ImageJ: 25 years of image analysis. Nature Methods 9:671–675.
DOI:10.1038/nmeth.2089

Shan X, Wang H, Zhang S, et al. 2003. Accumulation and uptake of light rare earth elements in a hyperaccumulator *Dicropteris dichotoma*. Plant Science 165:1343–1353.
DOI:10.1016/S0168-9452(03)00361-3

Sherman J. 1955. The theoretical derivation of fluorescent X-ray intensities from mixtures. Spectrochimica Acta 7:283–306.
DOI:10.1016/0371-1951(55)80041-0

Silva VL, Mehltreter K, Schmitt JL. 2018. Ferns as potential ecological indicators of edge effects in two types of Mexican forests. Ecological Indicators 93:669–676.
DOI:10.1016/j.ecolind.2018.05.029

Solé VA, Papillon E, Cotte M, Walter Ph, Susini J. 2007. A multiplatform code for the analysis of energy-dispersive X-ray fluorescence spectra. Spectrochimica Acta Part B: Atomic Spectroscopy 62:63–68.
DOI:10.1016/j.sab.2006.12.002

Souza ENF, Hawkins JA. 2017. Comparison of Herbarium Label Data and Published Medicinal Use: Herbaria as an Underutilized Source of Ethnobotanical Information. Economic Botany 71:1–12.
DOI:10.1007/s12231-017-9367-1

Thomas WA. 1975. Accumulation of rare earths and circulation of cerium by mockernut hickory trees. Canadian Journal of Botany 53:1159–1165.
DOI:10.1139/b75-139

Utica G, Fabbrica E, Carminati M, et al. 2021. ARDESIA-16: a 16-channel SDD-based spectrometer for energy dispersive X-ray fluorescence spectroscopy. Journal of Instrumentation 16:P07057.
DOI:10.1088/1748-0221/16/07/P07057

van der Ent A, Echevarria G, Pollard AJ, Erskine PD. 2019a. X-Ray Fluorescence Ionomics of Herbarium Collections. Scientific Reports 9:4–8.
DOI:10.1038/s41598-019-40050-6

van der Ent A, Ocenar A, Tisserand R, Sugau JB, Echevarria G, Erskine PD. 2019b. Herbarium X-ray fluorescence screening for nickel, cobalt and manganese hyperaccumulator plants in the flora of Sabah (Malaysia, Borneo Island). Journal of Geochemical Exploration 202:49–58.
DOI:10.1016/j.gexplo.2019.03.013

van der Ent A, Baker AJM, Echevarria G, Simonnot MO, Morel JL. 2021. Agromining: Farming for Metals: Extracting Unconventional Resources Using Plants. Springer International Publishing, Cham

van der Ent A, Nkrumah PN, Purwadi I, Erskine PD. 2023. Rare earth element (hyper)accumulation in some Proteaceae from Queensland, Australia. Plant and Soil 485:247–257.
DOI:10.1007/s11104-022-05805-7

Vieira Lima L, Salino A, Kessler M, et al. 2023. Phylogenomic evolutionary insights in the fern family Gleicheniaceae. Mol Phylogenet Evol 184:107782.
DOI:10.1016/j.ympev.2023.107782

Wang Y, He L, Dong S, et al. 2023. Accumulation, translocation, and fractionation of rare earth elements (REEs) in fern species of hyperaccumulators and non-hyperaccumulators growing in urban areas. Science of The Total Environment 905:167344.
DOI:10.1016/j.scitotenv.2023.167344

Wei Z, Hong F, Yin M, et al. 2005. Structural differences between light and heavy rare earth elment binding chlorophylls in naturally grown fern *Dicranopteris linearis*. Biological Trace Element Research 106:279–297.
DOI:10.1385/BTER:106:3:279

Wei Z, Xia Z, Shu J, et al. 2022. Phylogeny and Taxonomy on Cryptic Species of Forked Ferns of Asia. Frontiers in Plant Science 12
DOI:10.3389/fpls.2021.748562

Wood BW, Grauke LJ. 2011. The Rare-earth Metallome of Pecan and Other Carya. Journal of the American Society for Horticultural Science 136:389–398.
DOI:10.21273/JASHS.136.6.389

Yuan M, Liu C, Liu W-S, et al. 2018. Accumulation and fractionation of rare earth elements (REEs) in the naturally grown *Phytolacca americana* L. in southern China. International Journal of Phytoremediation 20:415–423.
DOI:10.1080/15226514.2017.1365336

Zhang Z, Wang Y, Li F, Xiao HQ, Chai ZF. 2004. Distribution characteristics of rare earth elements in plants from a rare earth ore area. Journal of Radioanalytical and Nuclear Chemistry 252:461–465.
DOI:10.1023/a:1015834232718

FIGURE CAPTIONS

Figure 1. Violin charts representing the distribution of foliar concentrations obtained with the XRF instrument of Y, Mn, and Zn within the families Blechnaceae, Gleicheniaceae, Juglandaceae, and Phytolaccaceae.

Figure 2. (A) Distribution of specimens by foliar concentrations of Y for Blechnaceae, Gleicheniaceae, Juglandaceae, and Phytolaccaceae. Solid lines correspond to mean values and dashed lines correspond to median values. The specimens shown in these graphs are only those analysed with a concentration in Y >LOD. The black curves represent the density curves of the distributions. (B) Number of specimens belonging to different accumulation levels for Y (Table 1).

Figure 3. (A) Distribution of specimens by foliar concentrations of Mn and Zn for Blechnaceae, Gleicheniaceae, Juglandaceae, and Phytolaccaceae. Solid lines correspond to mean values and dashed lines correspond to median values. The specimens shown in these graphs are only those analysed with a concentration in Mn >LOD and a concentration in Zn >LOD. The black curves represent the density curves of the distributions. (B) Number of specimens belonging to different accumulation levels for Mn and Zn (Table 1).

Figure 4. Species-level representation of the number of specimens analysed with foliar concentrations of Y, Mn, and Zn >LODs. Only species containing at least one specimen with a foliar concentration of Y >LOD are shown. Percentages are calculated relative to the total number of specimens analysed for a given species. The accumulation categories refer to Table 1.

Figure 5. Synchrotron µXRF elemental maps showing the distributions of Mn, Br, and Zn in a frond of *Dicranopteris linearis* (specimen P01523962). The scan measures 91.33 × 32 mm, 20 µm step size, and 5 ms dwell

Figure 6. Synchrotron µXRF elemental maps showing the distributions of Mn, Br, and Zn in a frond of *Dicranopteris linearis* (specimen P01523962). The scan measures 15.88 × 4.15 mm, 6 µm step size, and 5 ms dwell

Table 1. Values of the concentrations of Y, Mn, and Zn relative to their different accumulation classes and the LOD values for these elements with the XRF instrument.

Class	Y (µg g^{-1})	Mn (µg g^{-1})	Zn (µg g^{-1})
Normal concentrations	<5	50–500	50–200
Accumulator	5–50	500–3000	200–3000
Hyperaccumulator	>50	>3000	>3000
LOD of XRF method	49–73	115–165	77–113

Table 2. Total number of specimens scanned and percentage of specimens above the XRF detection limits of Y, Mn, and Zn for each family.

	Specimens scanned	Y		Mn		Zn	
Blechnaceae	561	149	27%	27	5%	20	4%
Gleicheniaceae	1310	108	8%	477	36%	52	4%
Juglandaceae	1417	5	0.3%	582	41%	125	9%
Phytolaccaceae	1137	6	0.5%	354	31%	148	13%
Total	***4425***	***268***	***6.1%***	***1440***	***32.5%***	***345***	***7.8%***

Table 3. Concentrations of the different REEs in the samples analysed by ICP-AES. The concentrations are given in µg g^{-1} of dry matter. LQ corresponds to the limit of quantification of the ICP-AES instrument.

Family	Species	Specimen ID (barcode of the Paris herbarium sheet)	Sc	Y	La	Ce	Pr	Nd	Sm	Eu	Gd	Dy	Ho	Tm	Yb	Lu	LREEs	HREEs	Sum REEs
Blechnaceae	*B. orientalis*	P01576169	<LQ	661	391	477	121	612	157	53	235	160	18	5	39	5	2472	462	2934
		P01618486	<LQ	534	469	230	74	351	61	22	118	144	8	2	16	2	1741	290	2031
		P01571495	<LQ	657	1161	593	217	863	157	32	187	340	16	6	44	5	3680	598	4278
		P01619249	<LQ	1140	87	468	61	426	102	44	248	111	32	11	77	10	2328	489	2817
Gleicheniaceae	*D. flexuosa*	P01315784	<LQ	638	521	442	111	524	110	39	170	175	15	4	28	3	2385	395	2780
		P01315862	<LQ	132	62	140	14	143	44	15	63	31	<LQ	1	8	1	550	104	654
	D. linearis	P01315958	1	1130	1156	1037	311	1470	322	88	402	388	27	9	73	9	5515	908	6423
		P01474002	<LQ	699	198	629	99	657	163	54	271	119	14	3	26	3	2499	436	2935
		P00139656	<LQ	218	<LQ	5	<LQ	3	<LQ	1	10	9	2	2	8	1	227	32	259
	G. pectinata	P01316111	<LQ	564	99	210	43	203	44	32	123	76	16	4	30	3	1195	252	1447

Table 4. Concentrations of other elements in the samples analysed by ICP-AES. The concentrations are given in µg g^{-1} of dry matter.

Family	Species	Specimen ID (barcode of the Paris herbarium sheet)	Ca	Fe	K	Mn	P	Zn
Blechnaceae	*B. orientalis*	P01576169	4649	1592	10769	35	595	45
		P01618486	6046	2159	6609	20	710	54
		P01571495	6431	1812	10544	54	577	50
		P01619249	4080	1497	3956	66	1105	107
Gleicheniaceae	*D. flexuosa*	P01315784	3390	356	4947	198	229	37
		P01315862	669	15467	6714	70	605	92
	D. linearis	P01315958	4142	5404	8396	773	964	224
		P01474002	3501	3511	4915	1051	1500	325
		P00139656	1142	2415	6084	270	605	206
	G. pectinata	P01316111	676	953	7850	69	420	29

Figure 1

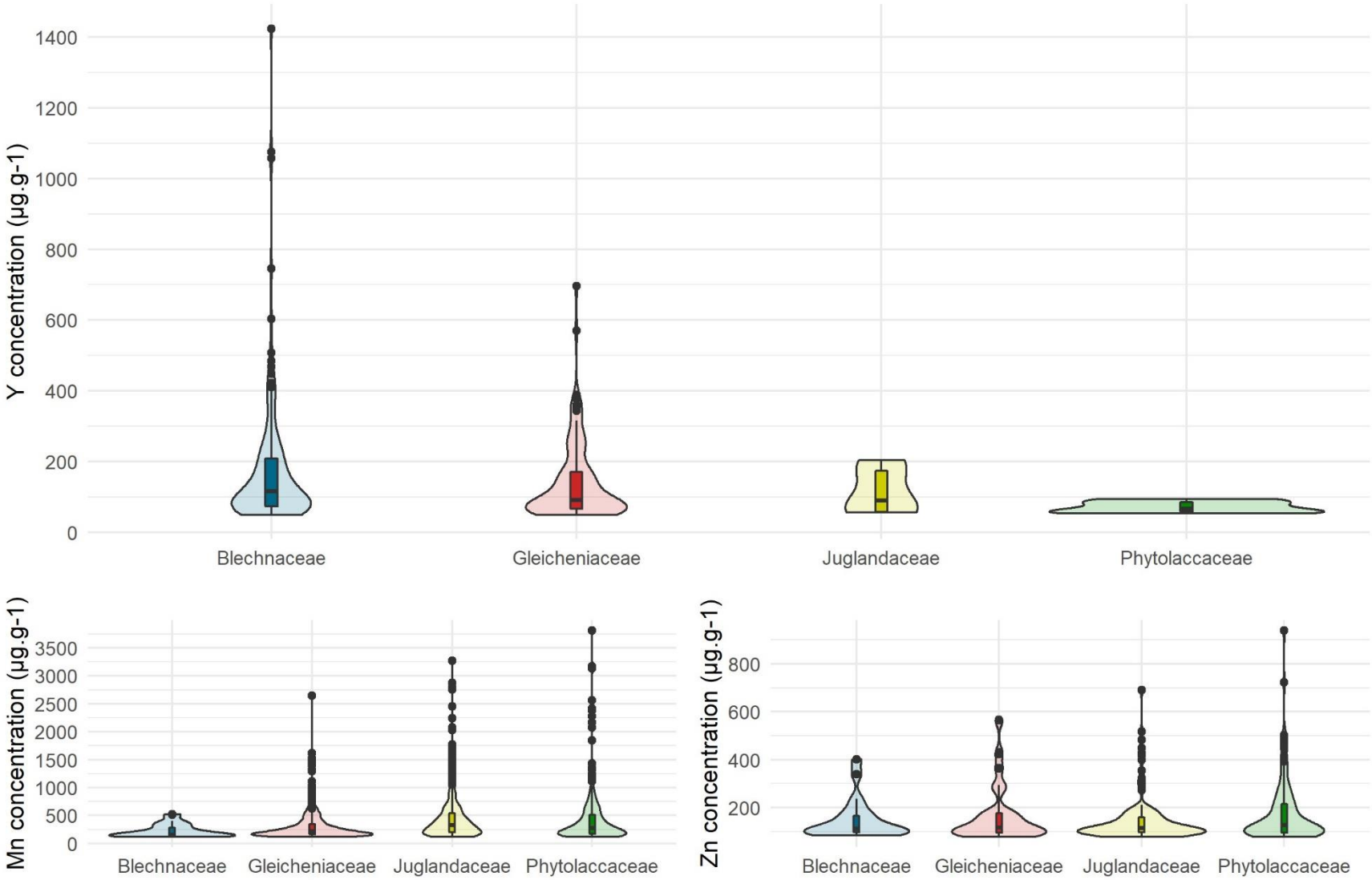

Figure 2

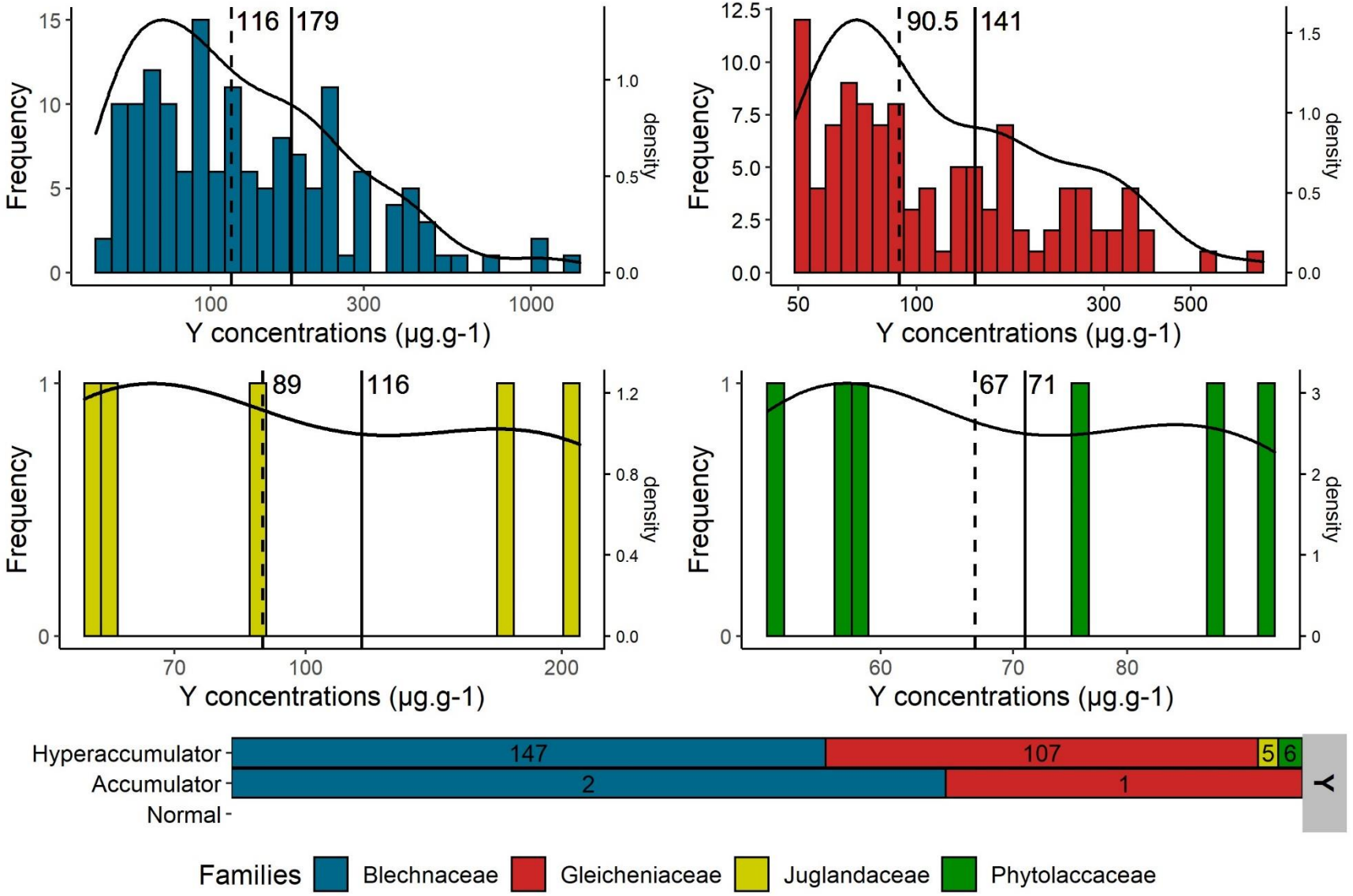

Figure 3

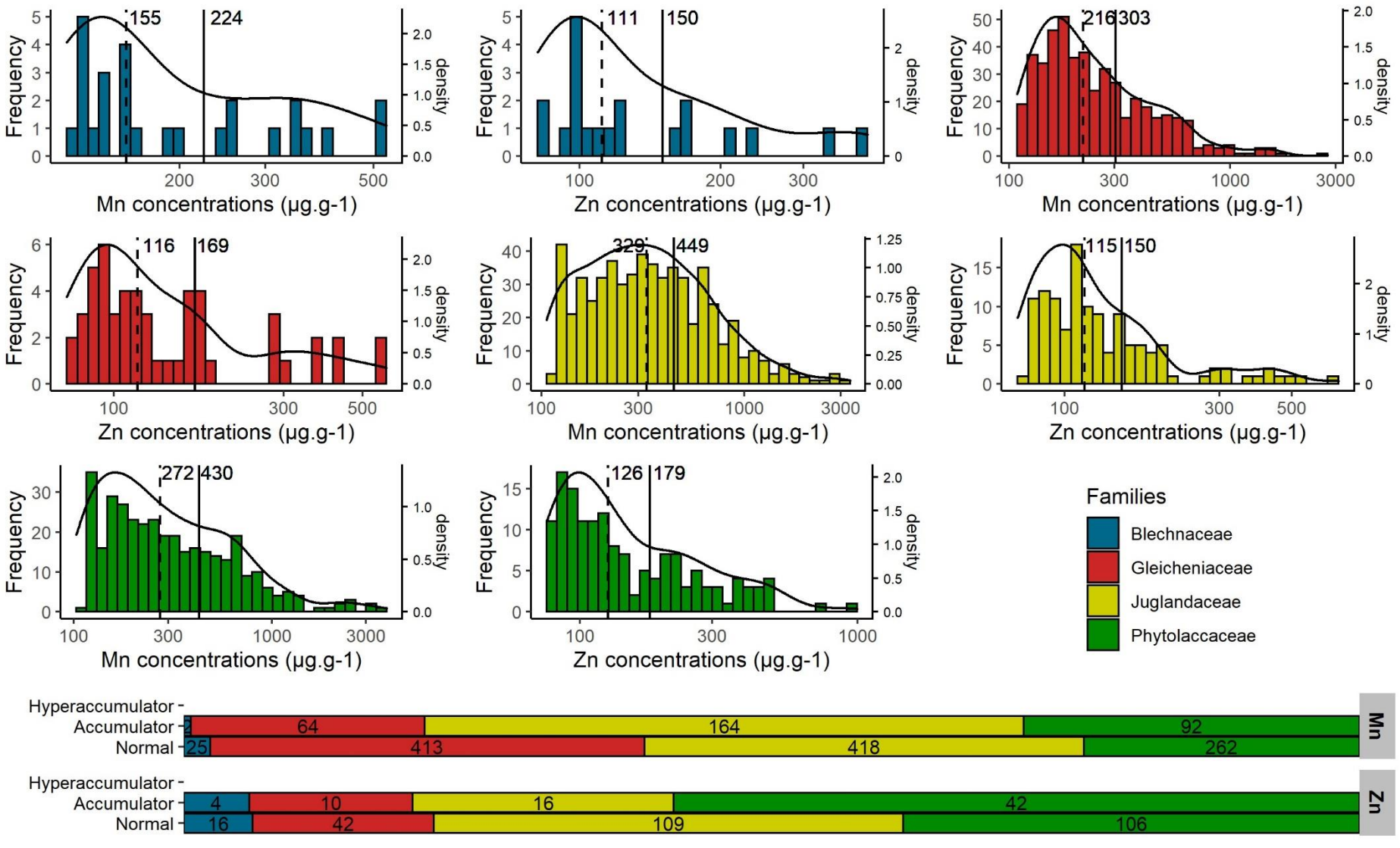

Figure 4

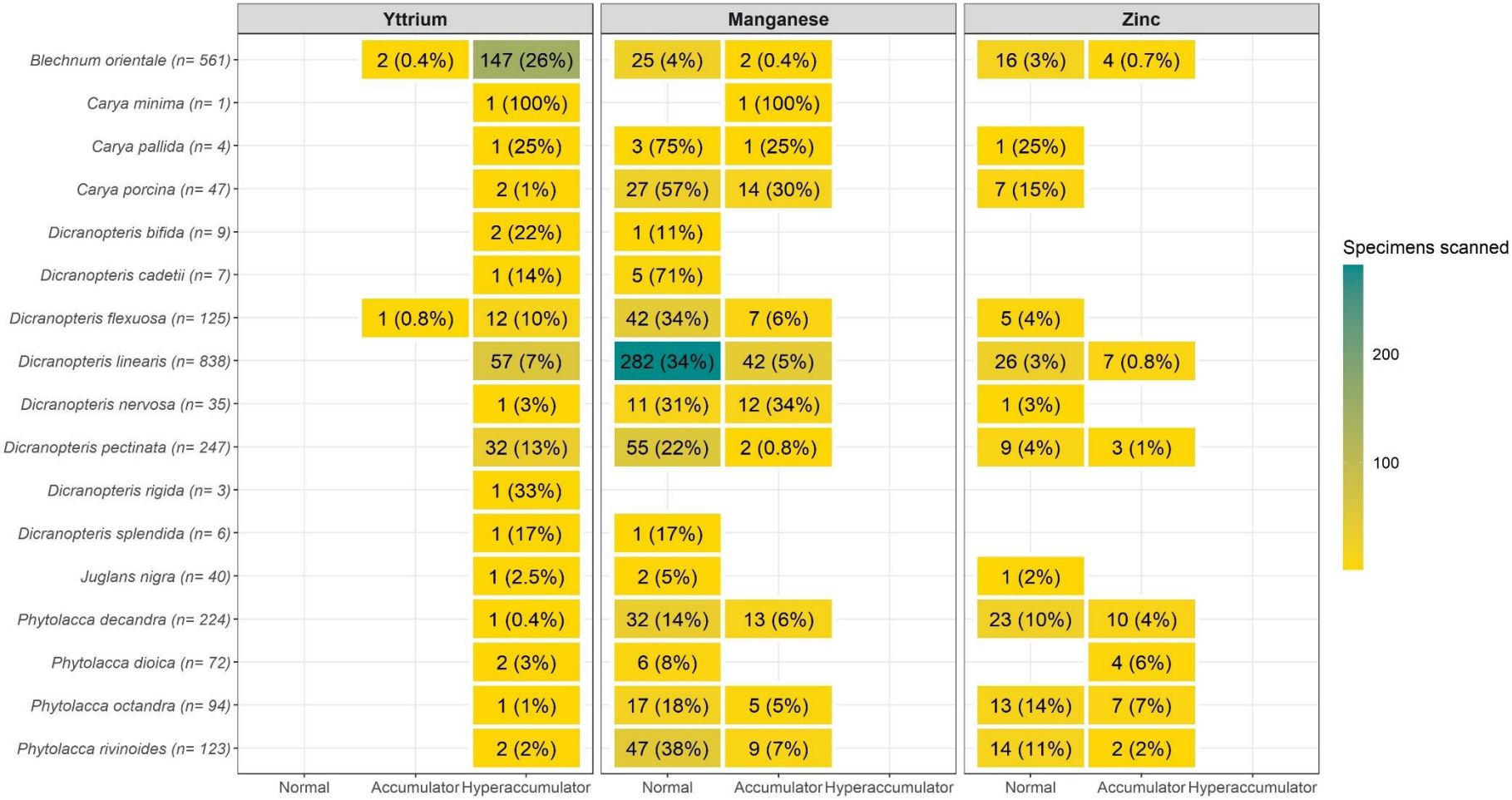

Figure 5

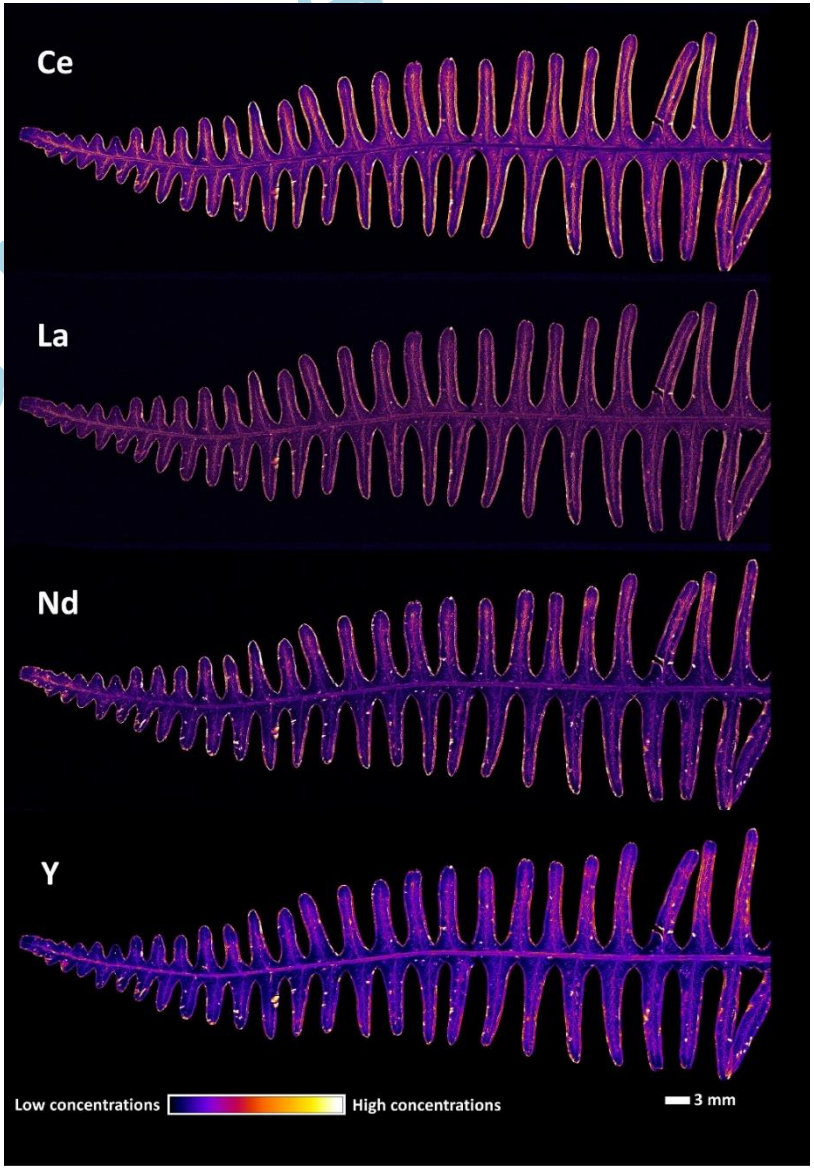

Figure 6